A role for Oncostatin M in the impairment of glucose homeostasis in obesity

Irene Piquer-Garcia[1*], Laura Campderros[2,3*], Siri D. Taxerås[1], Aleix Gavaldà-Navarro[2,3], Rosario Pardo[4], María Vila[4], Silvia Pellitero[1,5], Eva Martínez[1], Jordi Tarascó[6], Pau Moreno[6], Joan Villarroya[2,7], Rubén Cereijo[2,3], Lorena González[1], Marjorie Reyes[1], Silvia Rodriguez-Fernández[8], Marta Vives-Pi[8,5], Carles Lerin[9], Carrie M. Elks[10], Jacqueline M. Stephens[11], Manel Puig-Domingo[1,5], Francesc Villarroya[2,3], Josep A. Villena[4,5], David Sánchez-Infantes[1,3†]

[1] Department of Endocrinology and Nutrition, Germans Trias i Pujol Research Institute, Barcelona, Spain.

[2] Department of Biochemistry and Molecular Biomedicine, and Institute of Biomedicine, University of Barcelona, Barcelona, Spain.

[3]BiomedicalResearch Center (Red Fisiopatología de la Obesidad y Nutrición) (CIBEROBN), ISCIII, Madrid, Spain.

[4]Laboratory of Metabolism and Obesity, Vall d'Hebron Institut de Recerca, Universitat Autònoma de Barcelona, Barcelona, Spain.

[5]BiomedicalResearch Center (Red Fisiopatología de la Diabetes y enfermedades metabólicas) (CIBERDEM), ISCIII, Madrid, Spain.

[6]Department of Surgery, Germans Trias i Pujol Research Institute, Barcelona, Spain.

[7]Infectious Diseases Unit, Hospital de la Santa Creu i Sant Pau, Barcelona, Spain

[8]Immunology Section, Germans Trias i Pujol Research Institute, Barcelona, Spain.

[9]Endocrinology, Sant Joan de Déu Hospital, Barcelona, Spain.

[10]Matrix Biology Laboratory, Pennington Biomedical Research Center, Baton Rouge, Louisiana, USA.

[11]Adipocyte Biology Laboratory, Pennington Biomedical Research Center, Baton Rouge, Louisiana, USA.

*These authors contributed equally to this work.

†Correspondence:

David Sánchez-Infantes, PhD dsanchez@igtp.cat

Obesity and Type 2 Diabetes: Adipose Tissue Biology Group Leader

Germans Trias i Pujol Research Institute (IGTP), Campus Can Ruti, Carretera de Can Ruti, Camí de les Escoles s/n 08916 Badalona, Barcelona, Spain

Tel: (+34) 93 557 2832

Fax: (+34) 93 497 8654

Keywords: Oncostatin M, obesity, insulin resistance, inflammation.

Funding agencies

DS-I is Investigator of the Miguel Servet Fund from Carlos III National Institute of Health, Spain. This study was supported by grants CP15/00106 and FIS17/01455 from Instituto de Salud Carlos III and the Fondo Europeo de Desarrollo Regional (FEDER) to D.S.I., grants SAF2012-39484 and BFU2015-64462-R, and grant SAF2017-85722R fom the Ministerio de Economía y Competitividad (MINECO/FEDER) to J.A.V and to FV, respectively. C.M.E is supported by grant number K01 DK106307 from the National Institutes of Health.

Disclosure summary

I certify that neither I nor my co-authors have a conflict of interest as described above that is relevant to the subject matter or materials included in this Work.

Abstract

Context

Oncostatin M (OSM) plays a key role in inflammation, but its regulation and function during obesity is not fully understood.

Objective

The aim of this study was to evaluate the relationship of OSM with the inflammatory state that leads to impaired glucose homeostasis in obesity. We also assessed whether OSM immunoneutralization could revert metabolic disturbances caused by a high-fat diet (HFD) in mice.

Design

28 patients with severe obesity were included and stratified into two groups: 1) glucose levels < 100 mg/dL and 2) glucose levels > 100 mg/dL. White adipose tissue was obtained to examine OSM gene expression. Human adipocytes were used to evaluate the effect of OSM in the inflammatory response, and HFD-fed C57BL/6J mice were injected with anti-OSM antibody to evaluate its effects.

Results

OSM expression was elevated in subcutaneous and visceral fat from patients with obesity and hyperglycemia, and correlated with *Glut4* mRNA levels, serum insulin, HOMA-IR, and inflammatory markers. OSM inhibited adipogenesis and induced inflammation in human adipocytes. Finally, OSM receptor knockout mice had increased *Glut4* mRNA levels in adipose tissue, and OSM immunoneutralization resulted in a reduction of glucose levels and *Ccl2* expression in adipose tissue from HFD-fed mice.

Conclusions

OSM contributes to the inflammatory state during obesity and may be involved in the development of insulin resistance.

Introduction

Obesity has reached epidemic proportions worldwide, and its prevalence has doubled in the last 30 years. The prevalence of obesity affects more than 25% of the population, whereas a remarkable 60% of the population is overweight. Moreover, it has been estimated that approximately 350 million people have diabetes, representing almost 10% of the global population (1). White adipose tissue (WAT) is a crucial regulator of energy balance and glucose homeostasis, owing to its function as a lipid-storing and endocrine organ. Obesity is characterized by chronic, low-grade adipose tissue inflammation accompanied by an increased presence of various pro-inflammatory immune cells, including macrophages (2). The first wave of macrophage accumulation in WAT during the early phase of obesity is essential for healthy expansion and remodeling of adipose tissue (3). However, chronic infiltration of adipose tissue by macrophages, their polarization from a M2 anti-inflammatory state to a M1-like inflammatory state, and increased expression and secretion of pro-inflammatory cytokines have been shown to negatively impact systemic glucose homeostasis (4-7). Moreover, inflammatory processes may affect the browning capacity of WAT and by this means may also contribute to obesity-associated metabolic disease. Indeed, it has been demonstrated that the immune cell infiltration of subcutaneous WAT creates a deleterious inflammatory microenvironment that impairs the capacity of precursor cells to differentiate into thermogenically-active beige adipocytes (8). Understanding the cross talk between immune cells and adipocytes in the context of obesity is essential to define the pathological bases of metabolic diseases such as insulin resistance and type 2 diabetes.

In last decade, oncostatin M (OSM) has appeared as a relevant factor in the pathophysiology of obesity and other diseases (9). Indeed, it has been reported that OSM is an important target for breast cancer and inflammatory bowel disease (10, 11). In support of this notion, OSM immunoneutralization in animal models can improve these diseases (10, 11). OSM is a gp130 cytokine with its own specific receptor, OSMR, that heterodimerizes with gp130 and mediates the majority of OSM actions (12). OSM shares substantial sequence identity with leukemia inhibitory

factor (LIF) (13) and can modulate a variety of biological processes, such as liver development and regeneration (14, 15), hepatic insulin resistance and steatosis (16), inflammation (17), and cardiomyocyte dedifferentiation and remodeling (18). OSM has been also reported to promote bone formation and to inhibit adipogenesis (19-24).

Previously, we demonstrated that OSM was overproduced in WAT under obese conditions in mice and humans (25). In addition, we observed that OSM treatment inhibited adipogenesis in brown adipose tissue (BAT) and browning of WAT *in vitro* and *in vivo* using murine models (26). In this study, we aimed to decipher the role of OSM in promoting the inflammatory state that underlies the altered glucose homeostasis in obesity. We also addressed the therapeutic potential of OSM immunoneutralization to prevent an impairment in glucose homeostasis *in vivo*.

Materials and Methods

Human subject characteristics

45 patients with severe obesity (body mass index > 35 kg/m2 and comorbidities including type 2 diabetes, hypertension or dyslipemia) were included in our cohort (Table 1). Patients were stratified into two groups according to their fasting glycemia: normoglycemic patients (glucose<100 mg/dL) (n=26) and hyperglycemic patients (glucose >100 mg/dL) (n=19). All patients were evaluated by the same endocrinology specialist (S.P) according to criteria for bariatric surgery formulated in Spanish Position Statement between Obesity, Endocrinology, Diabetes and Surgery Societies (27). Demographic and clinical data, including age, history of diabetes, and hypertension were recorded for all subjects.

Serum samples and tissues

Serum samples from the study subjects were collected after a 12h fasting period. All samples were stored at -80ºC in the Biobank of the Health Sciences Research Institute Germans Trias i Pujol Foundation.

Twenty-one of these 45 patients with obesity (10 normoglycemics (9 females/1 male) and 11 hyperglycemics (6 females/5 males) were selected to analyze subcutaneous and visceral WAT (sWAT and vWAT, respectively) samples from the abdominal region. These 21 patients were chosen according to the following criteria: a) available sWAT and/or vWAT biopsis to isolate the required amount of high-quality RNA, and b) clinical history with at least body weight and blood glucose data available (see Flow chart in Supplementary Figure S1 (28)). WAT samples from patients with obesity were collected during bariatric surgery and immediately frozen at -80ºC.

The Institutional Ethics Committee, in accordance with the Declaration of Helsinki, approved the study (PI16-025). All participants gave their written informed consent before collecting clinical data and samples.

Human serological analysis

Glucose and insulin levels, and lipid profiles (total cholesterol, HDL and LDL cholesterol, and triglycerides) were measured in the certified core clinical laboratory at the hospital. Leptin and HMW-adiponectin levels were measured by specific ELISA kits (EZHL-80SK, Merck-Millipore and RYD-DHWAD0, R&D Systems, respectively). The homeostatic model assessment of insulin resistance (HOMA-IR) was calculated with the following formula:

$$HOMA - IR = \frac{\left[Glucose\,\frac{mg}{dL}\right] * \left[Insulin\,\frac{\text{m.u.int}}{dL}\right]}{405}$$

Human SGBS cell differentiation and OSM treatment

Simpson Golabi Behmel Syndrome (SGBS) human preadipocytes (29) were differentiated to adipose cells as reported previously (30). Briefly, pre-adipocytes were maintained with DMEM/F12 supplemented with 10% heat inactivated FBS, 32 µM biotin and 16 µM pantothenic acid. To induce their differentiation, cells were incubated with DMEM/F12 supplemented with 32 µM biotin, 16 µM pantothenic acid, 25nM dexamethasone, 500 µM IBMX, 2 µM rosiglitazone, 10 µg/mL transferrin, 20 mM insulin, 100 nM cortisol and 0.2 nM T3 for 7 days and incubated with DMEM/F12 supplemented with 32 µM biotin, 16 µM panthotenic acid, 10 µg/mL transferrin, 20 µM insulin, 100 nM cortisol and 0.2 nM T3 for 7 additional days or until they reached more than 90% of

differentiation. Where indicated, cells were treated with 1 mM cAMP (Sigma-Aldrich) and 1nM OSM (R&D systems; reference 295-OM-CF) for 6 and 24h or with 1 µM CL316.243 (Cayman Chemicals) for 24h for acute response. Cells were treated with 1 nM OSM (~22ng/ml) during all differentiation processes for chronic response studies.

Gene expression analyses

Total RNA was extracted from whole adipose tissue or cells using a column-affinity based methodology (NucleoSpin RNA II; Macherey-Nagel, Duren, Germany). 500 ng of total RNA were retrotranscribed into cDNA using random hexamer primers and Multiscribe reverse transcriptase (TaqMan reverse transcription reagents, Thermo Fisher Scientific), following the manufacturer's instructions. Platinum Quantitative PCR SuperMix-UDG with ROX reagent (Themo Fisher) was used as master mix reagent and expression levels of each gene of interest were assessed with the specific TaqMan probes (Thermo Fisher) (Supplementary Table S1 (28)). Gene expression was calculated by ΔΔCt method and expressed in arbitrary units.

Animal studies

Immunoneutralization study

Animals used in this study included male C57BL/6J mice fed a high-fat diet (HFD; 60% kcal from fat, Research Diets Inc, D12492). A group of male mice fed a low-fat diet (10% kcal from fat, Research Diets Inc, D12450B) was used as a diet control (n= 6). HFD feeding began at 8-weeks of age and extended for a 9-week period. After 7 weeks of HFD feeding, animals were randomized into two groups: a) mice receiving intraperitoneal injections twice a week for a total dose of 250 µg anti-OSM antibody (PA547022; Thermo Fisher Scientific, United States) over 2 weeks (n= 6); b) mice receiving intraperitoneal injections twice a week for a total dose of 250 µg IgG non-specific antibody (PA547309; Thermo Fisher Scientific, United States) over 2 weeks (n= 6) (Supplementary Figure S2 (28)). Antibody dosing was based on a previous study performed by Lapeire *et al* (10).

Tissues were collected for total RNA analysis. All experimental procedures were approved by the Institutional Animal Care and Use Committee of the University of Barcelona following the

principles outlined in the Declaration of Helsinki for animal experimental investigation.

Glucose and insulin tolerance tests

For glucose tolerance test (GTT), mice were first fasted for 12 h. Then, they were injected intraperitoneally with glucose (2 g/Kg body weight) and blood glucose was measured at 0, 30, 60, 90 and 120 min. For insulin tolerance tests (ITT), mice were fasted for 5 h and then blood glucose was measured at 0, 30, 60, 90 and 120 min following an intraperitoneal injection of insulin (0.85 U/Kg of body weight). Glucose levels were measured in blood using an ELITE glucometer (Bayer, Spain).

Rodent serological analysis

Blood was obtained by cardiac puncture and centrifuged at 2000 rpm for 10 minutes at 4 ºC to obtain serum. Total cholesterol and triglyceride levels were quantified by using commercial kits based on the Trinder method (FAR Diagnostics, Verona, Italy). Non-esterified fatty acids (NEFA) were measured in serum samples with the NEFA-C kit (Wako Chemicals, Neuss, Germany). Insulin levels were determined with an ultra-sensitive mouse insulin ELISA kit (Crystal Chem, Zaandam, The Netherlands).

Osmr ^{FKO} mice

Male adipocyte-specific *Osmr* knockout (*Osmr*^{FKO}; n=6) and littermate floxed control (*Osmr*$^{fl/fl}$; n=6) mice on a C57BL/6J background, generated as described previously (31, 32), were fed a HFD (45% calories from fat; Research Diets; D12451) for 20 weeks, beginning at 6 weeks of age. Body weights were obtained weekly. After 20 weeks of feeding, blood glucose levels were obtained after a 4-hour fast, mice euthanized, and inguinal white adipose tissue (iWAT) collected for gene expression analyses.

Western blotting

50 mg of frozen white adipose tissue were homogenized in 150ul of a buffer containing 50mM TrisHCl pH 7.4, 150 mM NaCl, 1.5mM $MgCl_2$, 1 mM EDTA, 1% v/v Triton X-100, protease inhibitor cocktail (Roche) and phosphatase inhibitors (2mM sodium orthovanadate, 1mM sodium pyrophosphate, 10mM sodium fluoride). Lysates were centrifuged at 16,000 g at 4°C for 10 min.

Protein concentration was measured using the bicinchoninic acid (BCA) protein assay as specified by the manufacturer (Pierce, Thermo Fisher Scientific, Rockford, IL). 30µg of protein of each sample (n=3) were resolved by SDS-polyacrylamide 12% gels and transferred onto PVDF membranes (GE Healthcare, Chicago, IL). Membranes were blocked for 1 h at room temperature (RT) in PBS 1x with 0.1% Tween 20 and 5% skimmed milk. Primary antibody rabbit anti-p44/42 MAPK (Erk1/2) (9102; Cell Signaling Technology, Danvers, MA) 1/1000 and rabbit anti-Phospho-p44/42 MAPK (Erk1/2) (Thr202/Tyr204) (9101; Cell Signaling Technology) 1/1000 were incubated overnight at 4 ºC in PBS1x–0.1% Tween20-3% milk. After incubation with HRP-labelled secondary antibodies for 1h at RT in PBS1x–0.1% Tween20-3% milk, membranes were developed with the ECL system (Millipore-Merck, Burlington, MA) and chemiluminescence was measured using the LAS-3000 Imager (Fujifilm, Tokyo, Japan).

Histological analysis

Samples from WAT and BAT were fixed for 24 hours in 4% paraformaldehyde and embedded in paraffin. Paraffin blocks were cut into 5 µM sections and stained with hematoxylin and eosin (H&E) or used for immunohistofluorescence (IHF) staining. For IHF, rehydrated tissue sections were blocked with 3% BSA for 1h at room temperature. Preparations were then incubated with rat anti-mouse F4/80 (ab6640, Abcam) or goat anti-mouse CD206 (sc-34577, Santa Cruz Biotechnology, Santa Cruz, CA, USA) antibodies at a concentration of 10 $\mu g \cdot mL^{-1}$ followed by AlexaFluor 488-conjugated anti-rat or anti-goat IgG secondary antibodies (Thermo Fisher Scientific). Immunofluorescence signals were visualized under a fluorescence microscope (Leica). All signal counting procedures were performed by an observer blinded to the identity of samples.

Statistical analysis

Data are presented as mean ± SD or SEM (for humans and mice, respectively). Correlation analysis was implemented in SPSS Statistics (IBM). Normality of datasets was assessed with a Kolmogorov-Smirnoff test. Statistical significance was determined using a two-tailed t-test, a Mann-

Whitney U-test for non-parametric data, or a one-way ANOVA with Tukey's post-hoc test for more than two groups. $p<0.05$ was established as the statistical significance threshold for all analyses.

Results

OSM expression is elevated in sWAT and vWAT from hyperglycemic patients with obesity and correlates with Glut4, Ccl2, Nos2 and Pai1 mRNA levels

We previously demonstrated that OSM expression is elevated in conditions of severe obesity (25). However, the relationship between adipose tissue OSM expression and glycemia in patients with obesity has not been explored. Here, in an independent cohort of patients with severe obesity (Table 1), we analyzed whether OSM levels were correlated with altered glucose homeostasis in obesity, by comparing WAT OSM expression levels in hyperglycemic and normoglycemic patients. We observed that the mRNA levels of *OSM* were increased in sWAT and vWAT from hyperglycemic patients when compared to *those* in normoglycemic patients (Figure 1A). We also found a decrease in *Glut4* mRNA levels in WAT from patients with hyperglycemia (Figure 1B), and an inverse correlation with OSM mRNA levels (Figure 1C). Moreover, *OSM* expression correlated with transcript levels of some inflammatory molecules, such as *Ccl2, Tnfα, and Col6* (a marker of fibrosis) (Figure 1D-F), although no correlation with *Nos2* and *Pai1* expression was observed (Figures 1G and 1H).

In addition, we found direct positive correlations between *OSM* expression and insulin levels or HOMA-IR in sWAT but not in vWAT, and no correlation with body weight (Figure 2), suggesting that *OSM* expression in sWAT is associated with reduced insulin sensitivity in obesity. After performing a linear regression analysis with all the clinical parameters and adjusting by sex and age, correlations between OSM expression and insulin or HOMA-IR were not maintained. However, body weight was as an independent predictor of OSM gene expression (Supplementary Table S2 (28)).

OSM inhibits differentiation and induces inflammatory markers in human adipocytes

The effects of OSM on human adipogenesis have not been previously addressed. Therefore, human cells were treated with human recombinant OSM during differentiation (chronic exposure) or after cells were completely differentiated into mature adipocytes (acute exposure). As shown in Figure 3A, OSM treatment caused complete inhibition of adipogenesis. OSMRβ was expressed in both preadipocytes and mature adipocytes, with higher levels in preadipocytes (Figure 3B). In addition, acute treatment of mature adipocytes with OSM produced significant increases in *Ccl2*, *Pai1* and *Il-6* expression, and a significant decrease in *Glut4* at 24 hours (Figure 3C). Conversely, *Col6* and *Adipoq* gene expression levels were not significantly regulated by OSM treatment (Figure 3D).

Osmr^{FKO} *mice exhibit enhanced sWAT Glut4 mRNA levels compared to Osmr*$^{fl/fl}$ *controls*

Since OSM was elevated in the sWAT of patients with obesity and insulin resistance, and considering that OSM treatment decreased *Glut4* gene expression and increased inflammatory gene expression in human adipocytes, we next sought to evaluate the *in vivo* effects of diminished adipocyte OSM signaling on these parameters. To accomplish this, we used HFD-fed *Osmr*^{FKO} and *Osmr*$^{fl/fl}$ control mice. Importantly, body weights did not significantly differ between genotypes (Figure 4A). We did observe a significant increase in sWAT *Glut4* mRNA levels in *Osmr*^{FKO} mice compared to floxed control mice (Figure 4B), but transcript levels of inflammatory markers *Ccl2*, *Nos2* and *Pai1* remained unchanged (Figure 4C-E).

OSM immunoneutralization reduces Ccl2 expression in white and brown adipose tissue and normalizes glucose levels in diet-induced obese mice

We aimed to evaluate the effect of systemic OSM inhibition on WAT and glucose homeostasis. To achieve this goal, we administered an anti-OSM antibody for 2 weeks to mice that had been previously fed a HFD for 7 weeks. Lower levels of phospho p44/42 mitogen-activated

protein kinases (MAPKs) (p-ERK1/2), a signaling kinase activated by OSM, were observed in mice treated with anti-OSM (Supplementary Figure S3 (28)), demonstrating the efficiency of the treatment of mice with the anti-OSM antibody in preventing the activation of OSM-induced signaling pathway. In addition, we measured *OSM* and *OSMR*β gene expression and other pro and anti-inflammatory markers (*Tnfα, Nos2, and Il10*) and F4/80 levels by immunostaning in the eWAT of the 3 groups of mice (low-fat control diet, HFD anti-IgG and HFD anti-OSM antibody). Significant increases in *Osm*, *Tnfα* and *Il10* mRNA levels were observed in the HFD anti-IgG group, in addition to more F4/80 positive cells, while these increases were not significant in mice treated with anti-OSM antibody. These results demonstrate the partial benefit of anti-OSM antibody injection, which was sufficient to ameliorate general inflammatory response (Supplementary Figure S4 (28)).

Mice treated with the anti-OSM antibody exhibited lower glucose levels compared to the anti-IgG control group, in a similar extent to those present in mice fed a low-fat control diet (Figure 5A). Insulin levels showed a tendency to be higher in the anti-OSM antibody group compared to anti-IgG group and were significantly different than those observed in the low-fat control diet group (Figure 5B). Consistent with our *in vitro* data in human adipocytes, we observed that administration of an anti-OSM neutralizing antibody lowered *Ccl2* gene expression in eWAT and BAT of HFD-fed mice when compared to HFD-fed mice given the anti-IgG control antibody (Figures 5D and E). There were no differences in *Ccl2* expression in iWAT (Figure 5F). PAI1 expression increased in BAT with HFD and was normalized after OSM immunonetralization (Figure 5G), and no changes were found in WAT (Figures 5 H and I). Moreover, we did not observe changes in *Glut4* mRNA levels in iWAT from the 3 groups of study (Figure 5C). As expected, compared to mice fed a low-fat control diet, HFD-fed mice exhibited impaired glucose homeostasis (Suplemmentary Figure S5A) in close association with the development of obesity. Despite changes in basal glucose levels, treatment with anti-OSM antibody for two weeks did not induce any significant changes in glucose tolerance or insulin sensitivity compared with mice treated with anti-IgG antibody (Suplemmentary Figure S5A-B). Similarly, no differences in body weight or food intake were observed between IgG or anti-OSM

antibody-treated mice (Supplementary Figure S5C-D (28)). WAT and BAT weights were similar in both groups of HFD-fed mice, independently of treatment (Supplementary Figures S6A-C (28)). Moreover, no differences in *Pparγ* expression were observed in WAT and BAT from either group on HFD (Supplementary Figures S6D-F (28)), suggesting that adipogenesis was not affected by the neutralizing antibody. Consistent with this, adipocyte size in iWAT and eWAT depots was not affected by the treatments (data not shown).

Discussion

In this study, we report for the first time that OSM is differentially expressed in adipose tissue from hyperglycemic patients with obesity when compared to normoglycemic patients with a similar degree of obesity. In addition, we demonstrate that OSM inhibits human adipogenesis, reduces *Glut4* expression, and induces an inflammatory state in human adipocytes. The inhibitory effect of OSM on adipocyte differentiation has been previously reported in different conditions (19-24). Here, we link the capacity of OSM to impair adipogenesis with its potential role to promote an inflammatory state, contribuiting to the development of insulin resistance in obesity. Consistent with these observations, our data in animal models also demonstrate that *Osmr*^{FKO} mice show higher levels of *Glut4* compared to floxed controls, and that OSM immunoneutralization reduces inflammatory markers and decreases basal glucose levels in obese mice.

In the last decade, the enigmatic concept of "healthy obesity" has emerged in the field of metabolism (33). Whether healthy obesity is only a transient state in the progression towards metabolic disease is controversial and still a subject of intense debate. But, it is clear that some patients maintain normal glucose homeostasis in presence of obesity (34). Metabolically healthy patients with obesity are characterized by the absence of metabolic complications such as dyslipidemia, insulin resistance, and unfavorable inflammatory profiles (35). Whereas dietary composition and physical activity are factors that have been related to metabolic health in patients with obesity, numerous studies have provided evidence implicating chronic inflammation,

particularly in adipose tissue, as a key factor in determining an unfavorable metabolic outcome in patients. Indeed, higher levels of pro-inflammatory cytokines, including C-reactive protein, Il-6, Pai1 or Tnfα have been reported in unhealthy obesity compared with healthy obesity (36, 37).

In this regard, OSM, a cytokine from the Il-6 family, is produced by adipose tissue and highly expressed in WAT of mouse models of diet-induced and genetic obesity, as well as in humans with obesity (25). Our data showing that increased expression of OSM in WAT correlates with markers of metabolic disease, including decreased *Glut4* expression, hyperglycemia, hypersulinemia, and increased HOMA-IR in patients with obesity, suggests that OSM is a marker of unhealthy obesity.

The correlation of OSM levels in sWAT with glycemia, but not with body weight, in patients may seem somewhat paradoxical given the finding that OSM negatively acts on precursor cells to inhibit adipocyte differentiation *in vitro*. A regulatory role of OSM on adipose tissue mass is supported by studies in mice lacking whole-body OSM receptor (OSMRβ), which show increased fat mass (38, 39). However, in humans, the causal factors underlying fat accretion in obesity are yet to be fully determined, and genetic or lifestyle factors (hypercaloric diets, sedentarism) may override the protective effect of OSM. On the other hand, the lack of any effect on body weight and adipose tissue mass in mice treated with an anti-OSM neutralizing antibody could be explained by: a) the short period of treatment (only two weeks), which was likely not sufficient to observe the effects of impaired adipocyte differentiation on WAT mass , or b) the dosage used.

A major finding of our study is the observation of direct correlations between OSM and inflammatory markers such as the monocyte chemoattractant, *Ccl2*, in WAT of patients. These results are in accordance with our previous data and with studies by other researchers that reported a pro-inflammatory role for OSM (10, 11, 25). Moreover, the effect of OSM in inducing these inflammatory genes in human adipocytes strongly suggests a potential role for OSM in adipose tissue inflammation in patients.

In addition, OSM downregulates *Glut4* in WAT as demonstrated by the decreased WAT *Glut4* expression in patients with obesity and hyperglycemia, the inverse correlation with *OSM* expression,

and the response to direct OSM exposure in human adipocytes. These results are suported by the elevation of sWAT *Glut4* expression in *Osmr*^{FKO} mice compared to floxed controls. These data suggest a potential contribution of this cytokine to impaired insulin sensitivity. This elevation in *Glut4* is unique to sWAT; as no differences were previously observed in vWAT *Glut4* expression in *Osmr*^{FKO} mice (31). This depot-specific expression pattern provides additional support for the possible protective role of sWAT, especially considering the increased vWAT inflammation observed in *Osmr*^{FKO} mice on both HFD and chow diets (31, 32).

Work by Elks *et al* using C57BL/6J mice demonstrated that OSM is primarily expressed in adipose tissue immune cells, and that OSMR is also expressed in cellular components of the adipose tissue immune system (32). Interestingly, however, *Osmr* expression increases only in adipocytes from HFD-fed mice (32). Further work using the adipocyte-specific *Osmr*^{FKO} mouse model showed significant increases in adipose tissue *Osm* expression in *Osmr*^{FKO} mice compared to *Osmr*$^{fl/fl}$ controls, along with increased adipose tissue inflammation. These findings suggest that since OSM could not bind OSMR on *Osmr*^{FKO} adipocytes, it was instead acting on other cell types within adipose tissue to promote inflammation and insulin resistance (31, 32).

Taking into account studies indicating that adipocyte OSMRβ signaling is important for adipose tissue homeostasis (31, 32), we examined the effects of OSM immunoneutralization on metabolic parameters in diet-induced obese mice. Regarding the inflammatory state, we observed a significant increase in *OSM*, *TNFα* and *Il10* mRNA levels in HFD-fed mice treated with IgG antibody, while this increase was not significant in HFD-fed mice treated with anti-OSM antibody compared to mice fed low-fat diet. The elevated levels of *Il10* in HFD-fed mice might be due to a compensatory mechanism against the increasing inflammatory process.

Moreover, anti-OSM treatment reduced the HFD-induced increase of *Ccl2* expression in vWAT and BAT, and also decreased *Pai1* expression in BAT. Further, glucose levels were normalized in HFD-fed mice after the OSM immunonetralization, although treatment with the anti-OSM antibody did not significantly alter whole body glucose tolerance or systemic insulin sensitivity.

Since we did not observe changes in *Glut4* expression, the mechanisms by which OSM neutralization normalized glucose levels in HFD-induced obese mice are still unclear. They may involve a reduction in the local adipose tissue inflammatory state and immune cell infiltration, as evidenced by reduction in transcript levels of chemoattractant and proinflammatory molecules, with a consequent improvement in adipocyte insulin sensitivity. However, the contribution of other tissues in response to treatment with this antibody cannot be disregarded. For example, the observed increase in insulin levels in anti-OSM treated mice could suggest direct effects on pancreatic β-cells. Moreover, a decrease in hepatic gluconeogenesis is also compatible with our observations. In this regard, OSM released by Kupffer cells in response to prostaglandin E2 has been shown to inhibit hepatic insulin signaling and to promote abnormal lipid accumulation (16).

Similar to studies by Komori et al. (38-40), we are confident that OSM is secreted from non-adipocyte cells in white adipose tissue under obese conditions in mice and humans, and that the expression of the *OSM* receptor, *OSMRβ*, is elevated in adipose tissue in conditions of obesity. However, a clear divergence between our observations and those reported in by Komori includes the primary function of OSM signaling in adipose tissue. Our results demonstrate that OSM has proinflammatory roles on adipocytes, including induction of *Ccl2* and *Pai-1*, and that levels of *OSM* in adipose tissue inversely correlated with glucose homeostasis parameters. Our observations supporting that elevated OSM levels in adipose tissue have negative effects, as part of an overall pro-inflammatory enhancement, are consistent with several studies by other laboratories. Lapeire *et al*. demonstrated recently that, of all the cytokines secreted by mammary adipose tissue, OSM is the most relevant secreted factor in stimulating breast cancer progression (10). Also, a study by Albiero *et al*. suggests that OSM antagonism is a strategy to restore bone marrow function in diabetes to combat the effects of elevated OSM levels produced in bone marrow macrophages in diabetics (41). We and others observed proinflammatory actions of OSM in adipocytes in mouse and human adipocytes (25, 42, 43). The fact that OSM is a strong inhibitor of adipogenesis (19-24) is consistent

with our proposal of OSM as a damaging factor on glucose homeostasis, as factors that limit fat cell expansion are commonly associated with metabolic dysfunction (7).

It is also important to point out that, for their studies *in vivo*, Komori et al. used a dose of recombinant OSM to treat mice (12.5 ng/g body weight, administered twice daily) (40) which is at least three to four orders of magnitude above the highest reported levels of circulating OSM in humans (42). A potential explanation for the differing conclusions could be related to the use of whole-body, constitutive, *Osmr* KO mice by Komori *et al*. *Osm* has well-known critical roles in liver development and hematopoiesis (14-18) and is expressed in many tissues during both embryonic development and adulthood in mice (42). OSMRβ-null mice had mature-onset obesity and insulin resistance (38), but this may be the result of multiple damaging events on early development, differentiation and cell programming beyond the actual role of OSM in adipose tissue when obesity develops in adulthood.

Since immunotherapy is being used to treat several inflammatory diseases (44), the practical implication of this study is to open the window for potential approaches targeting immunoregulation of adipose tissue in obesity to prevent and treat insulin resistance.

Regardless, our study presents some limitations, including the relatively low number of human adipose tissue samples and the lack of circulating OSM levels in these patients. Moreover, a polyclonal goat IgG might be immunogenic in mice and could act by neutralizing antibody responses over a two-week treatment period leading to a lack of effect due to poor drug pharmacokinetics. Further studies evaluating the effect of antibody treatment at earlier timepoints would be necessary to decipher whether OSM immunoneutralization could be a potential strategy to treat insulin resistance.

In conclusion, *OSM* is elevated in adipose tissue from patients with obesity and impaired glucose metabolism, and inversely correlates with *Glut4* expression in this tissue. Moreover, OSM promotes an inflammatory state during obesity, likely in part through the inhibition of adipogenesis, a direct reduction of the mRNA levels of *Glut4* and induction of the expression of inflammatory

markers. Finally, *Osmr*^{FKO} mice showed elevated levels of *Glut4*, and OSM immunoneutralization reduced adipose tissue *Ccl2* and *Pai1* expression in obese mice, and normalized glucose levels, demonstrating the negative action of OSM on glucose homeostasis. Further studies will be necessary to decipher whether blockage of OSM signaling can be a therapeutic target in preventing the development of T2D.

Acknowledgements

Samples from patients included in this study were provided by the IGTP HUGTP Biobank integrated in the Spanish National Biobanks Network of Instituto de Salud Carlos III (PT13/0010/0009) and they were processed following standard operating procedures with the appropriate approval of the Ethical and Scientific Committees.

References

1. WHO. Obesity and overweight. World Health Organization; 2017.

2. Apostolopoulos V, de Courten MP, Stojanovska L, Blatch GL, Tangalakis K, de Courten B. The complex immunological and inflammatory network of adipose tissue in obesity. *Mol Nutr Food Res*. 2016;60:43-57.

3. Pellegrinelli V, Carobbio S, Vidal-Puig A. Adipose tissue plasticity: how fat depots respond differently to pathophysiological cues. *Diabetologia* 2016;59:1075-1088.

4. Weisberg S, McCann D, Desai M, Rosenbaum M, Leibel R, Ferrante AJ. Obesity is associated with macrophage accumulation in adipose tissue. *J Clin Invest*. 2003;112:1796-1808.

5. Patsouris D, Li PP, Thapar D, Chapman J, Olefsky JM, Neels JG: Ablation of CD11c-positive cells normalizes insulin sensitivity in obese insulin resistant animals. *Cell Metab*. 2008;8:301-309.

6. Masoodi M, Kuda O, Rossmeisl M, Flachs P, Kopecky J. Lipid signaling in adipose tissue: Connecting inflammation & metabolism. Biochim Biophys Acta. 2015;1851:503-518.

7. Virtue S, Vidal-Puig A. Adipose tissue expandability, lipotoxicity and the Metabolic Syndrome--an allostatic perspective. Biochim Biophys Acta. 2010;1801:338-349.

8. Villarroya F, Cereijo R, Gavalda-Navarro A, Villarroya J, Giralt M. Inflammation of brown/beige adipose tissues in obesity and metabolic disease. *J Intern Med*. 2018;284:492-504.

9. Stephens JM, Elks CM. Oncostatin M: Potential Implications for Malignancy and Metabolism. *Curr Pharm Des*. 2017;23:3645-3657.

10. Lapeire L, Hendrix A, Lambein K, Van Bockstal M, Braems G, Van Den Broecke R, Limame R, Mestdagh P, Vandesompele J, Vanhove C, Maynard D, Lehuede C, Muller C, Valet P, Gespach CP, Bracke M, Cocquyt V, Denys H, De Wever O. Cancer-associated adipose tissue promotes breast cancer progression by paracrine oncostatin M and Jak/STAT3 signaling. *Cancer Res*. 2014;74:6806-6819.

11. West NR, Hegazy AN, Owens BMJ, Bullers SJ, Linggi B, Buonocore S, Coccia M, Gortz D, This S, Stockenhuber K, Pott J, Friedrich M, Ryzhakov G, Baribaud F, Brodmerkel C, Cieluch C, Rahman N, Muller-Newen G, Owens RJ, Kuhl AA, Maloy KJ, Plevy SE, Oxford IBDCI, Keshav S, Travis SPL, Powrie F. Oncostatin M drives intestinal inflammation and predicts response to tumor necrosis factor-neutralizing therapy in patients with inflammatory bowel disease. *Nat Med*. 2017;23:579-589.

12. Mosley B, De Imus C, Friend D, Boiani N, Thoma B, Park LS, Cosman D. Dual oncostatin M (OSM) receptors. Cloning and characterization of an alternative signaling subunit conferring OSM-specific receptor activation. *J Biol Chem*. 1996;271:32635-32643.

13. Rose TM, Lagrou MJ, Fransson I, Werelius B, Delattre O, Thomas G, de Jong PJ, Todaro GJ, Dumanski JP. The genes for oncostatin M (OSM) and leukemia inhibitory factor (LIF) are tightly linked on human chromosome 22. *Genomics* 1993;17:136-140.

14. Kamiya A, Kinoshita T, Ito Y, Matsui T, Morikawa Y, Senba E, Nakashima K, Taga T, Yoshida K, Kishimoto T, Miyajima A. Fetal liver development requires a paracrine action of oncostatin M through the gp130 signal transducer. *EMBO J*. 1999;18:2127-2136

15. Nakamura K, Nonaka H, Saito H, Tanaka M, Miyajima A. Hepatocyte proliferation and tissue remodeling is impaired after liver injury in oncostatin M receptor knockout mice. *Hepatology* 2004;39:635-644.

16. Henkel J, Gartner D, Dorn C, Hellerbrand C, Schanze N, Elz SR, Puschel GP. Oncostatin M produced in Kupffer cells in response to PGE2: possible contributor to hepatic insulin resistance and steatosis. *Lab Invest*. 2011;91:1107-1117.

17. Wallace PM, MacMaster JF, Rouleau KA, Brown TJ, Loy JK, Donaldson KL, Wahl AF. Regulation of inflammatory responses by oncostatin M. *J Immunol*. 1999;162:5547-5555.

18. Kubin T, Poling J, Kostin S, Gajawada P, Hein S, Rees W, Wietelmann A, Tanaka M, Lorchner H, Schimanski S, Szibor M, Warnecke H, Braun T. Oncostatin M is a major mediator of cardiomyocyte dedifferentiation and remodeling. *Cell Stem Cell*. 2011;9:420-432.

19. Walker, 2010. Oncostatin M promotes bone formation independently of resorption when signaling through leukemia inhibitory factor receptor in mice. J Clin Invest. 120:582- 592.

20. Guihard, 2012. Induction of osteogenesis in mesenchymal stem cells by activated monocytes/macrophages depends on oncostatin M signaling. Stem Cells. 30:762- 772.

21. Sato, 2014. Oncostatin M maintains the hematopoietic microenvironment in the bone marrow by modulating adipogenesis and osteogenesis. PLoS ONE. 9:e116209.

22. Song, 2007. Oncostatin M promotes osteogenesis and suppresses adipogenic differentiation of human adipose tissue- derived mesenchymal stem cells. J Cell Biochem. 101:1238- 1251.

23. Smyth, 2015. Oncostatin M regulates osteogenic differentiation of murine adipose- derived mesenchymal progenitor cells through a PKCdelta- dependent mechanism. Cell Tissue Res. 360:309- 319.

24. Song, 2007. Oncostatin M decreases adiponectin expression and induces dedifferentiation of adipocytes by JAK3- and MEK- dependent pathways. Int J Biochem Cell Biol. 39:439- 449.

25. Sanchez-Infantes D, White UA, Elks CM, Morrison RF, Gimble JM, Considine RV, Ferrante AW, Ravussin E, Stephens JM. Oncostatin m is produced in adipose tissue and is regulated in conditions of obesity and type 2 diabetes. *J Clin Endocrinol Metab*. 2014;99:E217-225.

26. Sanchez-Infantes D, Cereijo R, Peyrou M, Piquer-Garcia I, Stephens JM, Villarroya F. Oncostatin m impairs brown adipose tissue thermogenic function and the browning of subcutaneous white adipose tissue. *Obesity* 2017;25:85-93.

27. Sabench Pereferrer F, Dominguez-Adame Lanuza E, Ibarzabal A, Socas Macias M, Valenti Azcarate V, Garcia Ruiz de Gordejuela A, Garcia-Moreno Nisa F, Gonzalez Fernandez J, Vilallonga Puy R, Vilarrasa Garcia N, Sanchez Santos R, Sociedad Española de Cirugia de la O. Quality criteria in bariatric surgery: Consensus review and recommendations of the Spanish Association of Surgeons and the Spanish Society of Bariatric Surgery. *Cir Espan*. 2017;95:4-16.

28. Irene Piquer-Garcia, Laura Campderros, Siri D. Taxerås, Aleix Gavaldà-Navarro, Rosario Pardo, María Vila, Silvia Pellitero, Eva Martínez, Jordi Tarascó, Pau Moreno, Joan Villarroya, Rubén

Cereijo, Lorena González, Marjorie Reyes, Silvia Rodriguez-Fernández, Marta Vives-Pi, Carles Lerin, Carrie M. Elks, Jacqueline M. Stephens, Manel Puig-Domingo, Francesc Villarroya, Josep A. Villena, David Sánchez-Infantes. Data from: A role for Oncostatin M in the impairment of glucose homeostasis in obesity. GitHub depository. Deposited 6 of september 2019. https://github.com/dsanchez79/Spplemental-Material

29. Wabitsch M, Brenner RE, Melzner I, Braun M, Moller P, Heinze E, Debatin KM, Hauner H. Characterization of a human preadipocyte cell strain with high capacity for adipose differentiation. *Int J Obes Relat Metab Disord*. 2001;25:8-15.

30. Yeo CR, Agrawal M, Hoon S, Shabbir A, Shrivastava MK, Huang S, Khoo CM, Chhay V, Yassin MS, Tai ES, Vidal-Puig A, Toh SA. SGBS cells as a model of human adipocyte browning: A comprehensive comparative study with primary human white subcutaneous adipocytes. *Sci Rep*. 2017;7:4031.

31. Stephens JM, Bailey JL, Hang H, Rittell V, Dietrich MA, Mynatt RL, Elks CM. Adipose Tissue Dysfunction Occurs Independently of Obesity in Adipocyte-Specific Oncostatin Receptor Knockout Mice. *Obesity* 2018;26:1439-1447.

32. Elks CM, Zhao P, Grant RW, Hang H, Bailey JL, Burk DH, McNulty MA, Mynatt RL, Stephens JM. Loss of Oncostatin M Signaling in Adipocytes Induces Insulin Resistance and Adipose Tissue Inflammation in Vivo. *J Biol Chem*. 2016;291:17066-17076.

33. Eckel N, Li Y, Kuxhaus O, Stefan N, Hu FB, Schulze MB. Transition from metabolic healthy to unhealthy phenotypes and association with cardiovascular disease risk across BMI categories in 90 257 women (the Nurses' Health Study): 30 year follow-up from a prospective cohort study. *Lancet Diabetes Endo*. 2018;6:714-724.

34. Eckel N, Meidtner K, Kalle-Uhlmann T, Stefan N, Schulze MB. Metabolically healthy obesity and cardiovascular events: A systematic review and meta-analysis. *Eur J Prev Cardiol*. 2016;23:956-966.

35. Phillips CM. Metabolically healthy obesity: definitions, determinants and clinical implications. *Rev Endocr Metab Disord*. 2013;14:219-227.

36. Karelis AD, Faraj M, Bastard JP, St-Pierre DH, Brochu M, Prud'homme D, Rabasa-Lhoret R. The metabolically healthy but obese individual presents a favorable inflammation profile. *J Clin Endocrinol Metab*. 2005;90:4145-4150.

37. Koster A, Stenholm S, Alley DE, Kim LJ, Simonsick EM, Kanaya AM, Visser M, Houston DK, Nicklas BJ, Tylavsky FA, Satterfield S, Goodpaster BH, Ferrucci L, Harris TB, Health ABCS. Body fat distribution and inflammation among obese older adults with and without metabolic syndrome. *Obesity* 2010;18:2354-2361.

38. Komori T, Tanaka M, Senba E, Miyajima A, Morikawa Y. Lack of oncostatin M receptor beta leads to adipose tissue inflammation and insulin resistance by switching macrophage phenotype. The *J Biol Chem.* 2013;288:21861-21875.

39. Komori T, Tanaka M, Senba E, Miyajima A, Morikawa Y: Deficiency of oncostatin M receptor beta (OSMRbeta) exacerbates high-fat diet-induced obesity and related metabolic disorders in mice. *J Biol Chem.* 2014;289:13821-13837.

40. Komori T, Tanaka M, Furuta H, Akamizu T, Miyajima A, Morikawa Y. Oncostatin M is a potential agent for the treatment of obesity and related metabolic disorders: a study in mice. Diabetologia. 2015 Aug;58(8):1868-76.

41. Albiero M, Poncina N, Ciciliot S et al (2015) Bone Marrow Macrophages Contribute to Diabetic Stem Cell Mobilopathy by Producing Oncostatin M. Diabetes 64(8):2957–2968

42. Elks CM, Stephens JM (2015) Oncostatin m modulation of lipid storage. Biology (Basel) 4(1):151–160

43. Rega G, Kaun C, Weiss TW et al (2005) Inflammatory cytokines interleukin-6 and oncostatin M induce plasminogen activator inhibitor-1 in human adipose tissue. Circulation 111:1938–1945

44. Ignacio Catalan-Serra, Øystein Brenna. Immunotherapy in inflammatory bowel disease: Novel and emerging treatments. Hum Vaccin Immunother. 2018; 14(11): 2597–2611.

Figure legends

Figure 1: OSM expression is significantly elevated in sWAT and vWAT from hyperglycemic patients and correlates with *Glut4, Ccl2, Tnfα and Col6* gene expression.

Gene expression analysis of *OSM* (A) and *Glut4* (B) in sWAT and vWAT from normoglycemic patients with obesity and hyperglycemic patients with obesity. Correlations between *OSM* expression and *Glut4* (C), *Ccl2* (D), *Tnfα* (E), *Col6* (F), *Nos2* (G) and *Pai1* (H) gene expression. Expression levels are normalized to the reference gene *Ppia*. Data are presented as means ± s.e.m. (n= 21 samples, analytical assays performed in triplicate) * $p<0.05$ vs. normoglycemic obesity group.

Figure 2: *OSM* gene expression in sWAT but not in vWAT correlates with circulating insulin levels and HOMA-IR.

Correlations between *OSM* expression in sWAT and vWAT and insulin levels (A (n=14), D (n=15)), HOMA-IR (B (n=12), E (n=15)) and body weight (C (n=21), F (n=16)). Expression levels are normalized to the reference gene *Ppia*. Data are presented in arbitrary units as means ± s.e.m. (analytical assays performed in triplicate).

Figure 3: OSM inhibits human adipogenesis and induces a pro-inflammatory gene expression profile in mature human adipocytes.

A) Representative optical microscopy images from human preadipocytes treated with 1 nM OSM since day 1 of differentiation. *p<0.05 relative to control. B) Relative mRNA levels of *OSMRβ* in preadipocytes and mature adipocytes. C) Relative mRNA levels of *Ccl2*, *Pai1*, *Il-6* and *Glut4* in human mature adipocytes treated with 1nM OSM for 6 or 24 h. D) Relative mRNA levels of *Col6* and *Adipoq*. Expression levels are normalized to the reference gene *Ppia*. The bars represent means ± s.e.m. Each figure represents an experiment independently performed 3 times with 3 replicates per

sample. The mass unit concentration of 1 nM recombinant human OSM is ~22 ng/ml.

Figure 4: *Osmr*^{FKO} mice exhibit elevated *Glut4* mRNA levels, but no changes in inflammatory markers, compared to floxed controls

Body weight of Osmr^{FKO} mice and control littermates fed a HFD (A). Relative mRNA levels of *Glut4* (B), *Nos2* (C), *Ccl2* (D) and *Pai1* (E) in iWAT from HFD-fed *Osmr*^{FKO} mice and *Osmr*$^{fl/fl}$ controls. Data are presented in arbitrary units as means ± s.e.m. (n=6 mice per group and analytical assays performed in triplicate). Expression levels are normalized to the reference gene *Ppia*. * p<0.05 *Osmr*^{FKO} vs. *Osmr*$^{fl/fl}$ control mice.

Figure 5: OSM immunoneutralization decreases *Ccl2* expression in WAT and BAT and normalizes glucose levels.

Glucose (A) and insulin (B) levels in random fed animals. *Glut4* mRNA levels in iWAT (C). Relative mRNA levels of *Ccl2* (D, E, F) and *Pai1* (G, H, I) in WAT and BAT. The 3 groups correspond to: mice fed low fat control diet (control diet), mice fed a HFD and treated with unspecific IgG (HFD control), and mice fed a HFD and treated with anti-OSM Ab (HFD Ab). Data are presented in arbitrary units as means ± s.e.m. (n=6 mice per group and analytical assays performed in triplicate) * p<0.05 vs control diet.

Table 1. Anthropometric and metabolic parameters of human subjects.

Data are shown as mean ± (SD). LDL-Cho. HbA1c, glycated hemoglobin; HOMA-IR, Homeostatic model Assessment-insulin resistance; Low-density lipoprotein; HDL-Cho, High-density lipoprotein.*p value< 0.05

Table 1.- Anthropometric and metabolic parameters of human subjects.

	Normo (n=26)	**Hyper (n=19)**
	Mean ± SD	Mean ± SD
Age (years)	48±11	52±10
Sex (Female/Male)	20/6	14/5
History of T2D	no	7 T2D/12 pre-T2D
History of Hypertension (yes/not)	9/17	7/12
Weight (kg)	108 ± 19	117 ± 39
Height (cm)	163 ± 0.1	161 ± 0.3
Waist circumference (cm)	131 ± 11.2	146 ± 37.3*
Body mass index (kg/m^2)	41 ± 8.8	43 ± 10.8
Glucose (mg/dL)	91 ± 5	152 ± 46*
Insulin (m.u.int/L)	6.3 ± 3.4	7.7 ± 4.0
HbA1c (%)	5.3 ± 0.4	5.8 ± 0.2*
HOMA-IR (%)	1.4 ± 0.8	2.5 ± 1.3*
Triglyceride (mg/dL)	135 ± 41	161 ± 77
LDL-cholesterol (mg/dL)	95 ± 27	119 ± 23*
HDL-cholesterol (mg/dL)	41 ± 11	42 ± 10
Total cholesterol (mg/dL)	163 ± 34	191 ± 30*
HMW-adiponectin (ng/mL)	3016 ± 1849	2884 ± 1835
Leptin (ng/mL)	54.9 ± 25.1	42.8 ± 13.5

Data are shown as mean ± (SD). T2D, type 2 diabetes. HbA1c, glycated hemoglobin; HOMA-IR, Homeostatic model assessment-insulin resistance; Low-density lipoprotein; HDL-Cho, High-density lipoprotein; HMW-adiponectin, high molecular weight adiponectin.*p value< 0.05
Insulin (n= 20 normo and 10 hyper); HbA1c (n= 22 normo and 20 hyper); HOMA-IR (n= 20 normo and 10 hyper); Triglycerides (n= 25 normo and 11 hyper); LDL-cholesterol (n= 24 normo and 12 hyper); HDL-cholesterol (n= 24 normo and 12 hyper); Total cholesterol (n= 25 normo and 12 hyper); HMW-adiponectin (n= 13 normo and 8 hyper); Leptin (n= 13 normo and 8 hyper).

Figure 1

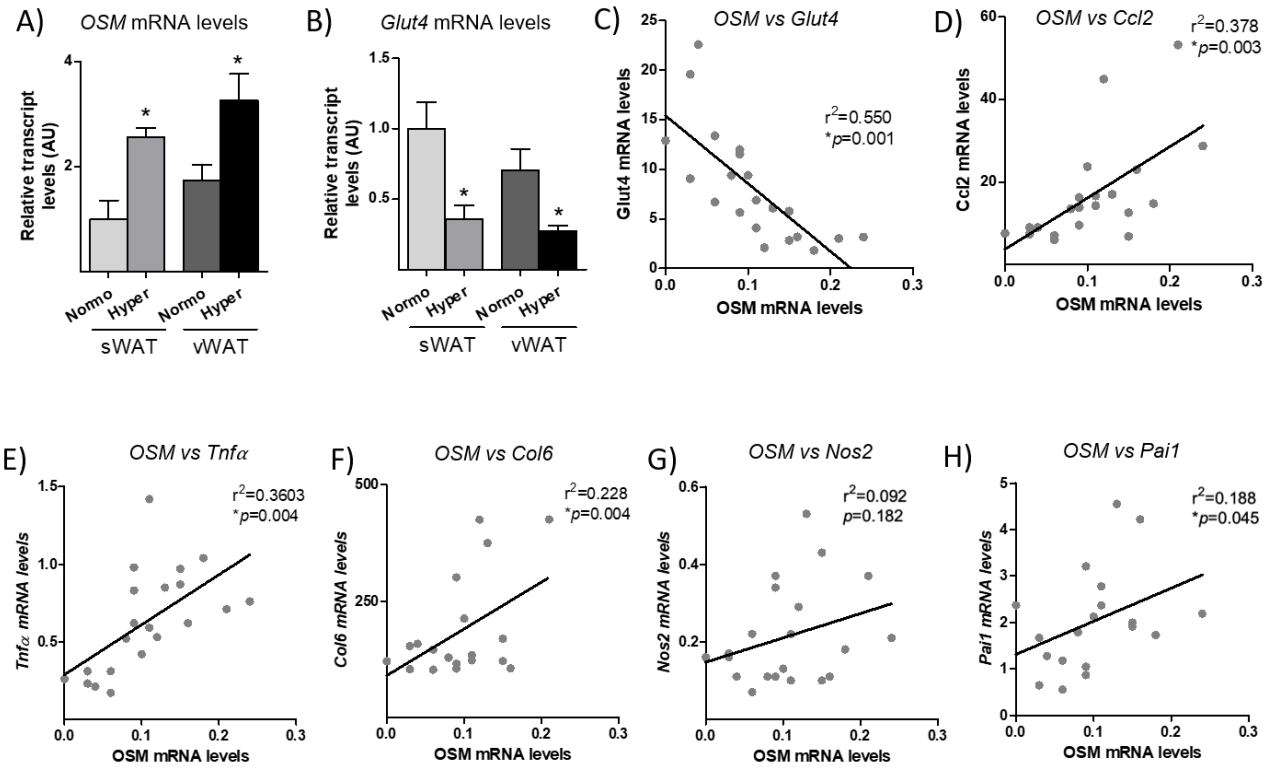

Figure 2

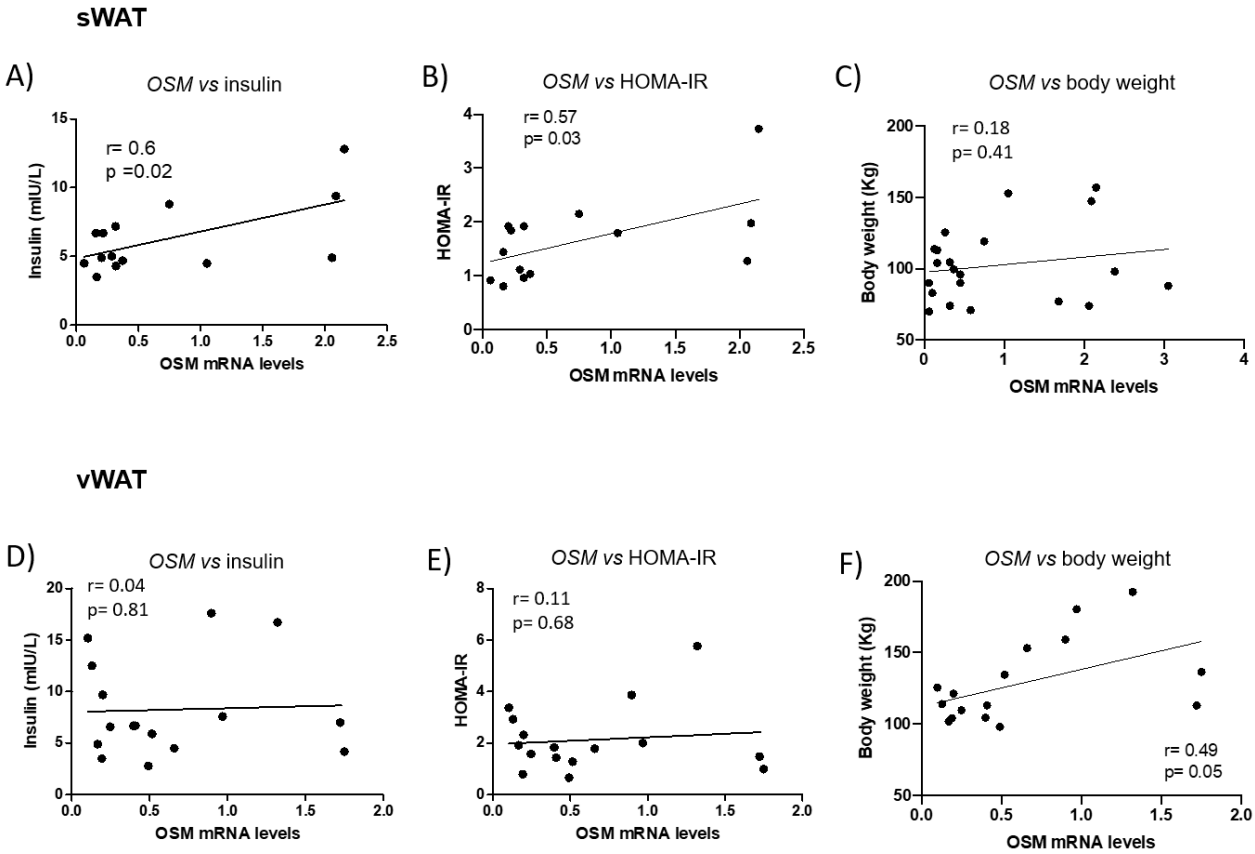

Figure 3

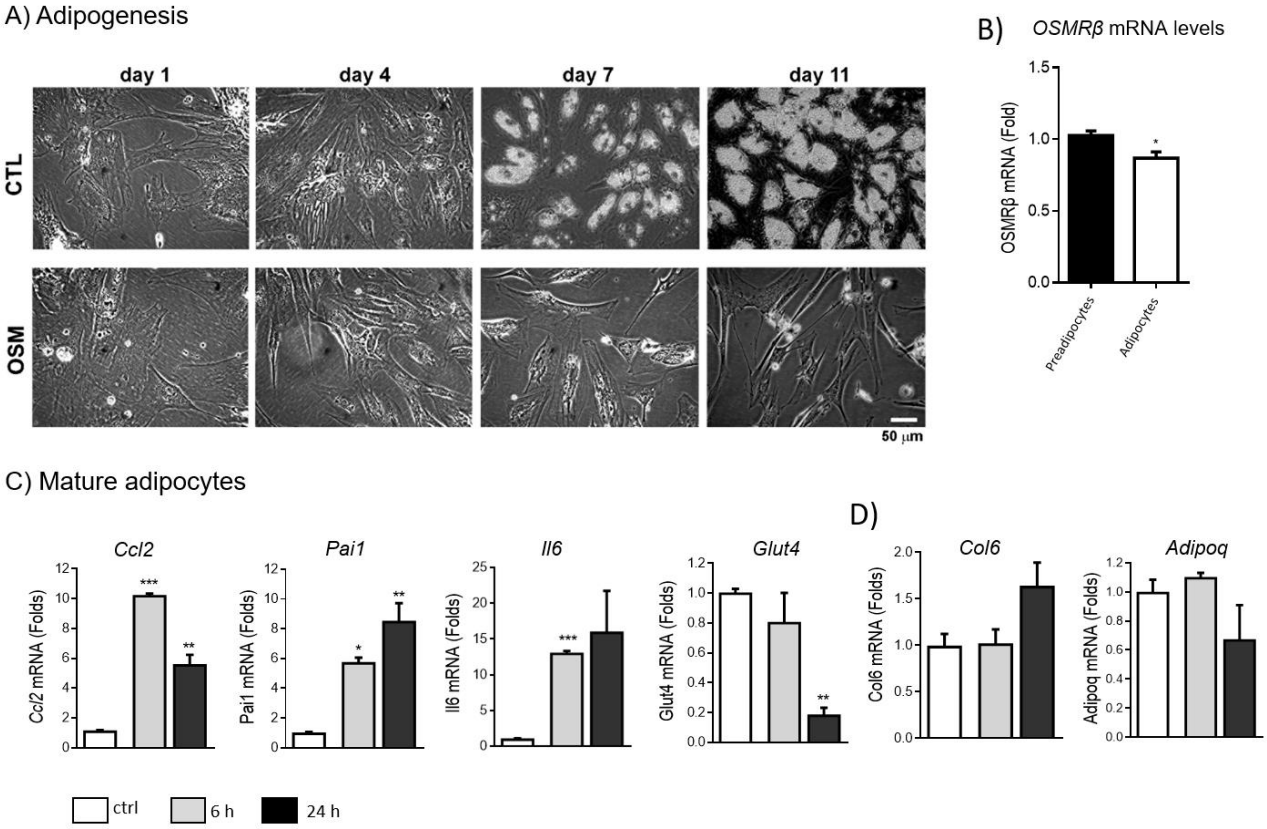

Figure 4

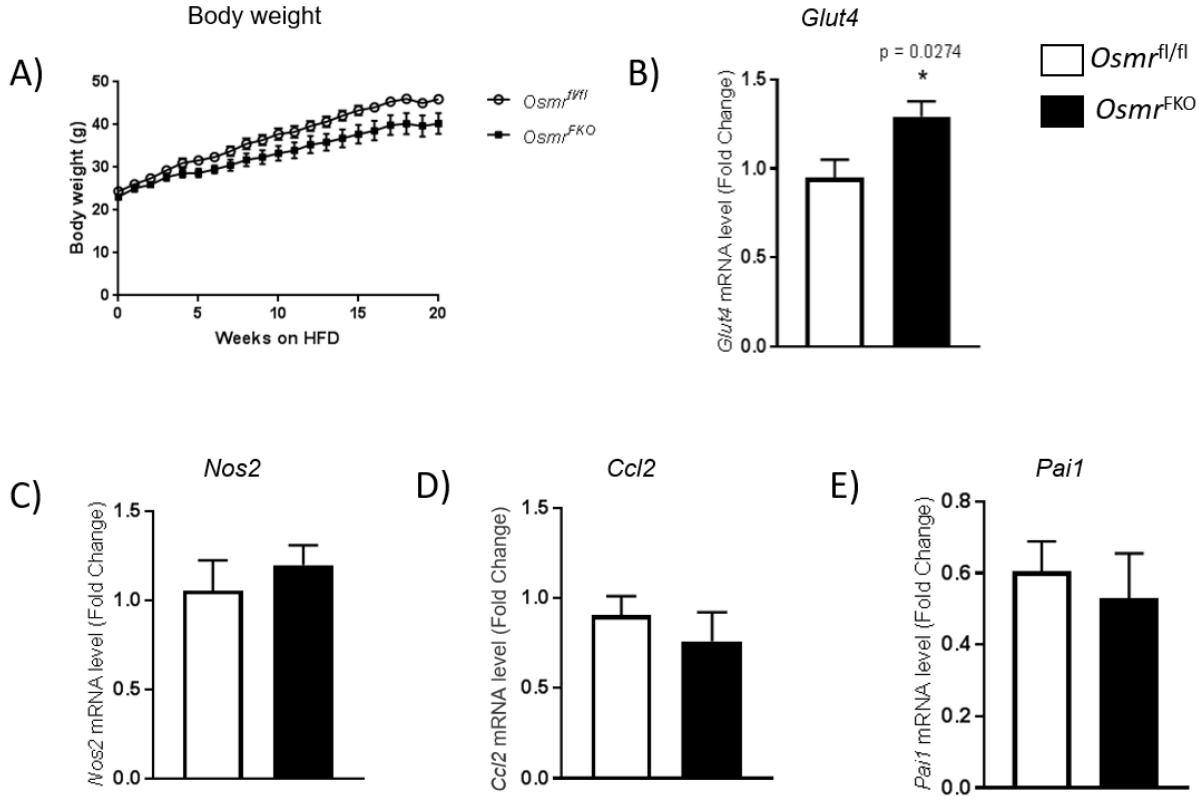

Figure 5